The 3rd International Conference on Sustainable Energy Information Technology (SEIT 2013)

Model-Based Fault-Tolerant Control to Guarantee the Performance of a Hybrid Wind-Diesel Power System in a Microgrid Configuration

Adriana Vargas-Martínez[a,b], Luis Ismael Minchala Avila[a,b], Youmin Zhang[a], Luis Eduardo Garza-Castañón[b], and Eduardo Robinson Calle Ortiz[c]

[a] Concordia University, 1455 de Maisonneuve Blvd., Montreal, H3G 1M8, Canada
{ad_varg@liveconcordia.onmicrosoft.com,ymzhang@encs.concordia.ca}
[b] Tecnológico de Monterrey, Campus Monterrey, Av. E. Garza Sada Sur 2501,
Monterrey, 64849, México {a00808366, legarza}@itesm.mx
[c] Engineering Research Center for Innovation and Development, Universidad Politécnica Salesiana,
Calle Vieja 12-30, Cuenca, Ecuador{ ecalle@ups.edu.ec}

Abstract

This paper presents a comparison of two different adaptive control schemes for improving the performance of a hybrid wind-diesel power system in an islanded microgrid configuration against the baseline controller, IEEE type 1 automatic voltage regulator (AVR). The first scheme uses a model reference adaptive controller (MRAC) with a proportional-integral-derivative (PID) controller tuned by a genetic algorithm (GA) to control the speed of the diesel engine (DE) for regulating the frequency of the power system and uses a classical MRAC for controlling the voltage amplitude of the synchronous machine (SM). The second scheme uses a MRAC with a PID controller tuned by a GA to control the speed of the DE, and a MRAC with an artificial neural network (ANN) and a PID controller tuned by a GA for controlling the voltage amplitude of the SM. Different operating conditions of the microgrid and fault scenarios in the diesel engine generator (DEG) were tested: 1) decrease in the performance of the diesel engine actuator (40% and 80%), 2) sudden connection of 0.5 MW load, and 3) a 3-phase fault with duration of 0.5 seconds. Dynamic models of the microgrid components are presented in detail and the proposed microgrid and its fault-tolerant control (FTC) are implemented and tested in the Simpower Systems of MATLAB/Simulink® simulation environment. The simulation results showed that the use of ANNs in combination with model-based adaptive controllers improves the FTC system performance in comparison with the baseline controller.

Keywords: Artificial Intelligence, Distributed Generation, Fault-tolerant Control, Microgrids, Model-based Control.

2. Introduction

Critical requirements on safety and operability issues with a desirable performance in technological systems, such as electrical, industrial, aircraft control, nuclear generation, etc., cause them to rely on complex control systems. Therefore, it is necessary to design control systems with fault-tolerance capabilities in order to improve the reliability and availability while providing a reasonable performance [1-3]. In smart grid (SG) applications, an emerging technology is the so-called microgrids, defined as small-scale low/medium voltage power systems with distributed energy sources (DES), storage devices and controllable loads, connected to the main power network or islanded. Microgrids are concerned with power generation near the consumers [4,5]. On the other hand, frequency and voltage regulation in interconnected electrical systems with multiple generation sources are main control challenges in distributed generation systems. Many different approaches have been studied and proposed for both grid-connected and islanded microgrid operation. Grid-connected operation relies on main grid parameters and the majority of contributions are related with volt-var strategies through the use of capacitor banks and flexible ac transmission system (FACTS), although advanced control strategies like adaptive controllers for voltage regulation at the generation unit are detailed in [6,7]. Islanded microgrid operation has generated the necessity of a frequency leader due to the high integration of the renewable energy sources (RES) whose intermittent characteristic complicates the use of traditional control schemes. Voltage and frequency regulation for isolated generators are studied in some research papers [8,9].

This paper presents a methodology of an FTC system which increases the fault-tolerant capability of a model-based adaptive controller, i.e. MRAC, by adding into its structure an ANN and a PID controller tuned by a GA. The MRAC structure has several advantages because it guarantees asymptotic output tracking and has a direct physical interpretation. In this research two different FTC schemes are proposed and are compared against the baseline controller, IEEE type 1 automatic voltage regulator (AVR). The first scheme uses a MRAC with a PID controller tuned by a GA to control the speed of the DE for regulating the frequency of the power system and uses a classical MRAC for controlling the voltage amplitude of the SM. The second scheme uses a MRAC with a PID controller tuned by a GA to control the speed of the DE; and a MRAC with an ANN and a PID controller tuned by a GA for controlling the voltage amplitude of the SM. In order to test the proposed schemes, different operating conditions of the microgrid and fault scenarios in the DEG were tested: 1) decrease of the DE actuator performance (40% and 80% actuator fault), 2) sudden connection of 0.5 MW load, and 3) a 3-phase fault with duration of 0.5 seconds. This paper is organized as follows: Section 2 describes the microgrid modelling; in Section 3, the proposed schemes are shown; Section 4 collects and discusses the experiments and results. Finally, Section 5 presents the conclusions.

3. Microgrid modeling

In order to test the controllers proposed in this research, a hybrid wind-diesel power system in an islanded microgrid configuration is developed first. A typical microgrid configuration, as stated, consists of DG units, controllable loads and storages. In the following subsections, detailed models of the network components used for the developed simulation testbed of the hybrid wind-diesel power system microgrid are presented.

3.1. Diesel engine generator

The diesel engine generator is composed of two machines: DE (prime mover) and synchronous generator which are described as follows.

For a complete dynamic simulation of the DE, a high order model would be required. However, for speed controller design purpose (frequency control of the grid), a simpler model will be enough. The actuator block is modeled by a first-order system with a gain K_a and a time constant T_a. On the other hand, the diesel engine block contains the combustion system and it is responsible to the movement of the pistons and in consequence the crankshaft will generate a torque $T(s)$ in the shaft. Some researches [10,11] use a time delay $e^{-\tau s}$ and a torque constant K_b for modeling this block. The flywheel block is an approximation of the complex inertia dynamics generated inside the machine, while the coefficient ρ

represents friction. The output, $x_2(t)$, represents the angular velocity of the machine's shaft, $d(s)$ is used for modeling load changes in rotor shaft, e.g. larger mechanical power demanded for the synchronous generator due to a connection of an electrical load. The continuous-time model of the DE is represented in state-space equations, as follows:

$$x_1(t) = -\frac{1}{T_a} x_1(t) + \frac{K_a}{(T_a)} u(t) \tag{1}$$

$$x_2(t) = \gamma K_b x_1(t-\tau) - \rho\gamma x_2(t) \tag{2}$$

In the synchronous generator the machine's shaft is driven by a prime mover, i.e., steam, hydraulic turbine or DE. The magnetic field produced by the field winding links the stator coils to induce voltage in the armature windings as the shaft is moved by the prime mover. A state-space model using the dynamic equations with *dq* (direct-quadrature) as frame reference, through a Park's transformation, for a pure resistive load R_L (a resistive load is used in the model, due to the fact that a microgrid is mainly resistive) connected into the synchronous machine is presented in [12] and is summarized as follows:

$$\mathbf{L}\frac{dx}{dt} = \mathbf{A}\mathbf{x} + \mathbf{B}v_F \tag{3}$$

$$\mathbf{x} = \begin{bmatrix} i_d \\ i_q \\ i_F \end{bmatrix} \quad \mathbf{A} = \begin{bmatrix} -(R_s + R_L) & \omega L\_s & 0 \\ -\omega L_s & -(R_s + R_L) & -\omega M_s \\ 0 & 0 & -R_F \end{bmatrix} \quad \mathbf{L} = \begin{bmatrix} L_s & 0 & M_s \\ 0 & L_s & 0 \\ M_s & 0 & L_F \end{bmatrix} \quad \mathbf{B} = \begin{bmatrix} 0 \\ 0 \\ 1 \end{bmatrix} \tag{4}$$

where $[i_d \quad i_q \quad i_F]^T$ are the *dq* stator and field currents, respectively; R_s and R_F are the stator and field resistances; L_s, L_m, and L_F are the stator, magnetizing, and field inductances, respectively; ω is the electrical speed; v_d and v_q are the *dq* stator voltages; and v_F is the field voltage which will be used as a control input.

3.2. Wind turbine generator

This subsection presents the model details of a wind energy conversion system (WECS), where a horizontal-axis wind turbine (WT) has been chosen as prime mover and an induction generator for energy conversion. This combination of WT and asynchronous machine is the most commonly wind turbine generator (WTG) found in commercial versions for generating powers ranging from a few kilowatts up to 3 MW. Combinations of several WTG form the so-called wind farms, with generation capacities up to 200 MW [13]. The operating condition of the WT is classified into three regimes: startup regime, sub-rated power regime and rated power regime. Dynamic simulation and the controller design are investigated in this work at rated power regime. To model the WT, the WT model proposed in [14,15] was selected, where a PID algorithm for blade pitch control is used. The WT model that is used here is with a lumped mass, i.e. it does not model the double mass phenomenon. The turbine is pitch controlled through the blade pitch angle, β. The power coefficient, C_p, characterizes the WT as a function of both tip speed ratio, $=\frac{\Omega R}{V_w}$, and β, where R is the WT rotor radius, Ω is the mechanical angular velocity of the WT rotor and V_w is the wind velocity.

$$C_p(\lambda,\beta) = \left[116\left(\frac{1}{\lambda+0.08\beta} - \frac{0.035}{\beta^3+1}\right) - 0.4\beta - 5\right] \times 0.5716e^{-21\left(\frac{1}{\lambda+0.08\beta} - \frac{0.035}{\beta^3+1}\right)} + 0.0039\lambda \tag{5}$$

The dynamic output is the mechanical torque T_m of the WT and is expressed as:

$$T_m = \frac{\rho A R C_p V_w^2}{2\lambda} \tag{6}$$

where ρ is the air density and A represents the swept area by the blades. On the other hand, for the induction generator, the electrical equations of induction generator model in the *dq* reference frame can be expressed as:

$$v_{qs} = r_s\, i_{qs} + \frac{\omega}{\omega_b}\psi_{ds} + \frac{p}{\omega_b}\psi_{qs} \tag{7}$$

$$v_{ds} = r_s\, i_{ds} + \frac{\omega}{\omega_b}\psi_{qs} + \frac{p}{\omega_b}\psi_{ds} \tag{8}$$

$$v'_{qr} = r'_r\, i'_{qr} + \frac{\omega-\omega_r}{\omega_b}\psi'_{dr} + \frac{p}{\omega_b}\psi'_{qr} \tag{9}$$

$$v'_{dr} = r'_r\, i'_{dr} + \frac{\omega-\omega_r}{\omega_b}\psi'_{qr} + \frac{p}{\omega_b}\psi'_{dr} \tag{10}$$

where ω_b is the base electrical angular velocity used to calculate the inductive reactance. The mechanical part is expressed in per unit as:

$$\frac{p}{\omega_b}\omega_r = \frac{1}{2H}(T_e - T_m) \tag{11}$$

$$T_e = \psi'_{qr}i'_{dr} - \psi'_{dr}i'_{qr} \tag{12}$$

3.3. Storage subsystem

An electrical battery is a collection of one or more electrochemical cells that convert stored chemical energy into electrical energy. A simple nonlinear Thevenin model has been adopted for mathematical modeling purposes in [16,17], whose aim is to design a discrete time estimator for the state of charge (SOC) of the battery. This model takes into account the dynamic response of the battery, which is influenced by the capacitive effects of the battery plates and by the charge-transfer resistance. In order to design control strategies for charge and discharge process of the battery, it is required to define state-space equations, leading to the following equations for the discharge process (charge process is similar, except for using R_C instead of R_d):

$$V_0 = R_d i(t) + \frac{1}{C}\int [i(t) + i_B(t)]dt \tag{13}$$

$$\frac{dV_p(t)}{dt} = -\frac{1}{R_d C}V_p(t) - \frac{1}{C}i_B(t) + \frac{1}{R_d C}V_0 \tag{14}$$

A linear (approximate) relationship between open circuit voltage and SOC is used in several research papers [16-18], leading to a simple equation for estimating battery's SOC:

$$S(t) = \frac{v_{oc}(t) - b}{a} \tag{15}$$

where b is the battery terminal voltage when $S(t) = 0$ and a is obtained knowing the value of b and v_{oc} at $SOC = 100\%$.

3.4. Microgrid configuration

Fig. 1 depicts the hybrid wind-diesel power system architecture that is to be controlled, where DC stands for distributed controller, CB stands for circuit breaker and ILVDC for intelligent low voltage dc breaker [19, 20]. System parameters used for simulation are shown in Table 1.
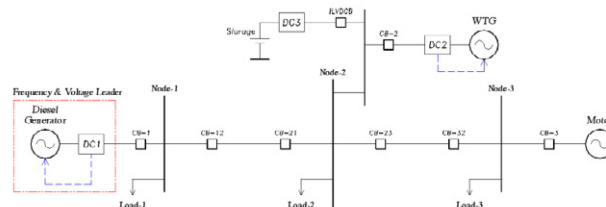

Figure 1. Hybrid wind-diesel power system architecture.

Table 1. Hybrid wind-diesel system parameters

Parameters	Value
SM power	3 MVA
Grid voltage	220 V
Grid frequency	60 Hz
WT nominal mechanical output	1.5 MW
WT max. power at base wind speed	0.85
Base wind speed	12 m/s
Load-1	2 MW
Load-2	0.5 MW
Load-3	0.4 MW

The overall control strategy of the microgrid is composed of three distributed controllers, this article just focused on DC1, each one with specific tasks: *DC1* implements the adaptive controllers proposed in this research, which are in charge of regulating both grid frequency and voltage amplitude. A DE is used as a prime mover that drags a SM generator at a constant speed. In an islanded configuration, the frequency is determined by the mechanical speed ω_m which is provided by the DE, while the voltage amplitude is set

by the synchronous generator field voltage. *DC2* is regarded with power generation control of the WTG. At this stage of the research, an unconstrained Model Predictive Control (MPC) for a limited range of the blade pitch angle, *β* between 0 to 10 degrees, has been designed. *DC3* controls a bi-directional dc-to-dc converter to manage battery charge and discharge. A classic PWM modulation control for the boost and buck converters are used. In addition, variable wind speed, ranging from 9 m/s to 18 m/s, was used during the simulation.

3. Proposed schemes

In the following section the two different FTC schemes based on MRAC developed in this research are described.

3.1. Classic MRAC for voltage control and MRAC plus PID controller tuned by GA for DE control (Scheme 1)

The MRAC implements a closed-loop controller that involves the parameters that should be optimized, in order to modify the system response to achieve the desired final value. The adaptation mechanism adjusts the controller parameters to match the process output with the reference model output. The reference model is specified as the ideal model behaviour that the system is expected to follow. The MRAC controller was designed using the Lyapunov theory methodology [21]. The mathematical procedure of this methodology starts with the error's equation:

$$e = y_{process} - y_{reference} = G_p u - G_r u_c \tag{16}$$

where *e*, $y_{process} = y_p$, $y_{reference}$, G_p, *u*, G_{ref} and u_c represent the error, process output, reference output, process model, process input, reference model and controller input, respectively. For a second order system, the implemented MRAC scheme has two adaptation parameters: adaptive feedfoward gain θ_1 and adaptive feedback gain θ_2. These parameters will be updated to follow the reference model. Then, the input is rewritten in terms of the adaptive feedforward and adaptive feedback gains as follows:

$$u = \theta_1 u_c - \theta_2 y_{process} \tag{17}$$

The Lyapunov stability theorem establishes the following: If there exists a function $V: R^n \rightarrow R$ being positive definite and its derivative is negative semidefinite, then the solution *x(t)=0* is stable. If *dV/dt* is negative definite the solution will be asymptotically stable. *V* denotes the Lyapunov function for the system. If:

$$dV/_{dt} < 0 \quad \text{and} \quad V(x) \rightarrow \infty \text{ when } \|x\| \rightarrow \infty \tag{18}$$

the solution is globally asymptotically stable. To design an MRAC controller using Lyapunov theory, the first step is to derive a differential equation for the error that contains the adaptation parameters. Then, a Lyapunov function and an adaptation mechanism need to be established to reduce the error to zero. The Lyapunov derivative function *dV/dt* is usually negative semidefinite. Therefore, determining the parameter convergence is necessary to establish persistently excitation and uniform observability on the system and the reference signal [22]. The proposed Lyapunov function is quadratic in tracking error and controller parameter estimation error because it is expected that the adaptation mechanism will drive both types of errors to zero. Based on previous research [23] the proposed Lyapunov function is (19):

$$V(e, \theta_1, \theta_2) = \frac{1}{2}\left(a_{1r}e^2 + \frac{1}{\gamma b_r}(b_r\theta_1 - b_r)^2 + \frac{1}{\gamma b_r}(b_r\theta_2)^2\right) \tag{19}$$

where b_r, γ and $a_{1r} > 0$. Eq. (19) will be zero when the error is zero and the controller parameters are equal to the desired values. The above Lyapunov function is valid if the derivative of this function is negative. Thus, the derivative of (19) is:

$$\dot{V} = -e\frac{d^2e}{dt^2} - a_{0r}e^2 + \frac{1}{\gamma}\left(b_r\theta_1 - b_r\right)\left(\frac{d\theta_1}{dt} + \gamma u_c e\right) + \frac{1}{\gamma}(b_r\theta_2)(\frac{d\theta_2}{dt} - \gamma y_p e) \tag{20}$$

And the selected adaptation parameters to ensure that error *e* will go to zero [21] are:

$$\frac{d\theta_1}{dt} = -\gamma u_c e \qquad \text{and} \qquad \frac{d\theta_2}{dt} = \gamma y_p e \tag{21}$$

Further details of this methodology can be found in [23].

3.1.1. MRAC combined with a PID controller tuned by a GA for DE control

To overcome the limitations of the simple MRAC structure (smaller fault accommodation threshold than the MRAC controller in combination with other structures), a classical PID controller is introduced in the feedforward part of the simple MRAC scheme (Fig. 2). The PID parameters were obtained by using a genetic algorithm (GA) pattern search to track the desired system trajectory with the MATLAB Optimization Toolbox. GA are searching and optimizing algorithms motivated by natural selection evolution. The simplest GA follows the next steps: Generate a random initial population of chromosomes (potential solutions), calculate the fitness of every chromosome in the population, apply selection, crossover and mutation and replace the actual population with the new population until the required solution is achieved.
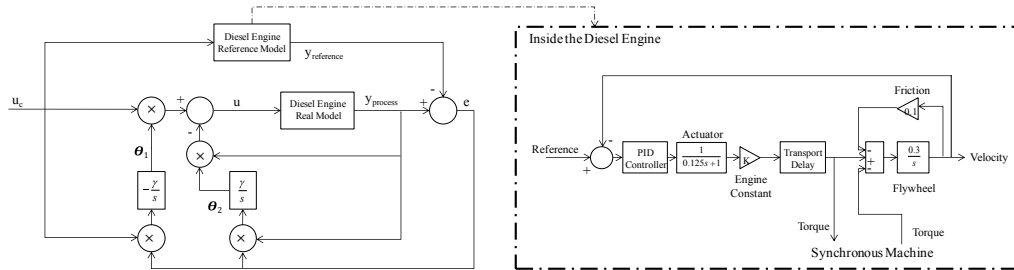

Figure 2. MRAC-PID to control the DE (a) left (b) right.

In this scheme, the desired closed-loop behaviour of the system is established through the model reference trajectory when there are no faults in the system. The parameters that need to be established for the desired optimization are shown in Table 2 (a). Then, the GA obtains the best parameter optimization (see Table 2 (b)).

Table 2. MATLAB® GA optimization toolbox parameters (a) and obtained best PID controller parameters using GA optimization (b)

(a)			(b)	
Parameters	Value		Parameter	Diesel Engine PID
Step Initial Value	0		Kp	3.8748
Step Final Value	1		Ki	2.6471
Step Time	0 s		Kd	1.9347
Rise time	7 s			
% Rise	90			
Settling Time	20 s			
% Settling	5			
% Overshoot	20			
% Undershoot	2			

3.1.2. Classic MRAC for voltage regulation in the microgrid

This controller uses the classical MRAC Lyapunov theory presented in section 3.1 and with this theory the following scheme is obtained (left side of Fig. 3).

3.2. MRAC combined with ANN plus PID controller for voltage control and MRAC with PID controller tuned by GA for DE control (Scheme 2)

This methodology integrates a MRAC with an ANN and a PID controller tuned by a GA in order to control the microgrid voltage and also uses a MRAC with a PID controller tuned by a GA to control the rotor shaft speed of the DE. The controller for the DE is the same as the one in section 3.1.1.

3.2.1. MRAC combined with an ANN and a PID controller tuned by a GA for voltage regulation in the microgrid

In order to increase fault accommodation threshold of the system, an ANN and a PID controller were integrated into the MRAC structure; these controllers have a feedforward architecture in order to obtain a robust FTC structure. In this structure, the PID controller helps to attenuate the overshoot, undershoot and also helps to obtain the desired settling time and rise time. On the other hand, the ANN controller will try

to attenuate the fault by helping the system to follow the desired reference trajectory. In addition, the controller structure adds robustness to the system; i.e. the PID helps to attenuate the signal, as it is shown in the right side of Fig. 3. To create and train the ANN controller, the original process inputs were introduced as well as the desired outputs. The created ANN is a two-layer feed-forward neural network with 20 sigmoid hidden neurons and a linear output neuron. To train the network, the Levenberg-Maquard backpropagation algorithm was used [24].
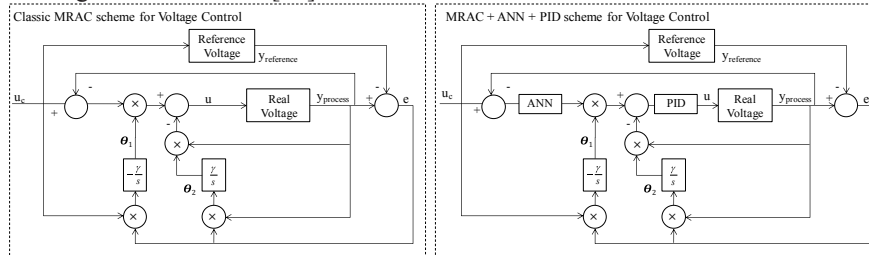

Figure 3. Classic MRAC scheme (left side) and MRAC plus ANN plus PID scheme (right side) for voltage regulation in the microgrid.

4. Experiments and results

In order to test the proposed schemes, different operating conditions of the microgrid and fault scenarios in the DEG were tested: 1) decrease of the DE actuator performance by 40% or 80% when 40 seconds have elapsed, 2) sudden connection of 0.5 MW load after 80 seconds of simulation, and 3) a 3-phase fault with duration of 0.5 seconds at 100 seconds of simulation. As mentioned in the introduction the two developed schemes are compared against the baseline diesel engine speed and voltage control that MATLAB has on its library, i.e. governor and PI controller for the rotor speed control and IEEE type 1 AVR for maintaining the voltage amplitude of the microgrid.
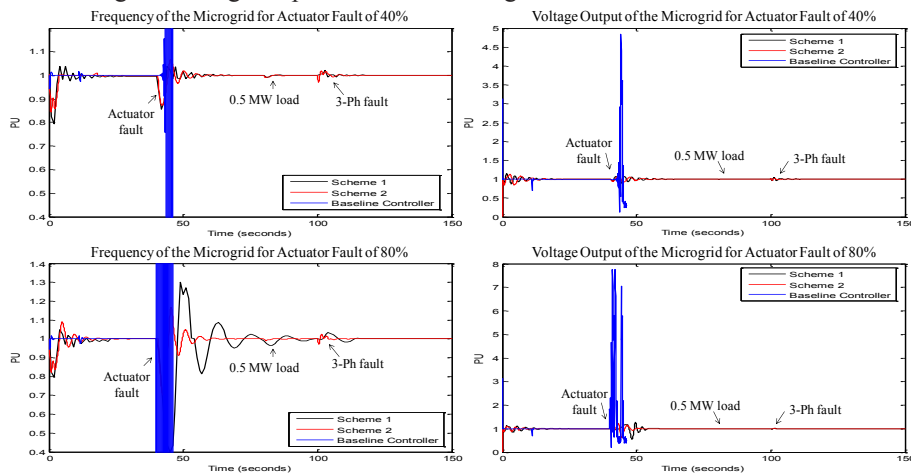

Figure 4. Comparison of the FTC schemes.

As shown in Fig. 4, the simulation results showed that the use of ANN in combination with MRAC improves the FTC capabilities, which can be clearly seen for the 80% of actuator fault case. It can be observed that the Scheme 2 was able to accommodate the actuator fault, in both cases when the actuator fault was 40% and 80%, the 0.5 MW load connection and the 3-Ph fault, leading to minor changes in voltage and frequency of the power system over than Scheme 1. On the other hand it can be observed that when the actuator fault increases to 80% Scheme 1 presented oscillation problems in the frequency of the microgrid for almost 80 seconds while Scheme 2 with very short and small transient period. In addition, it is clearly observed that the MRAC based schemes show a much better performance than the baseline controller due to its lack of fault tolerance, which causes system instability when the actuator fault occurs.

5. Conclusions

Although both designed Scheme 1 and Scheme 2 were able to accommodate the three tested scenarios when the actuator was 40%, it can also be observed that if more severe fault occurs in actuator Scheme 2 can accommodate the faults better. Compared with the baseline controller, the developed two controllers achieved a better performance in both voltage and frequency responses in the tested microgrid. It is achieved because the MRAC has an inherent capability to accommodate disturbances due to faults and load changes etc., and it is also relative easy for implementation. However, the use of only this type of controller has certain limitations. For this reason, a combination of MRAC with ANN has been proposed for guaranteeing system performance in the presence of unknown model dynamics, faults, and load variations with a better transient behavior and also disturbance rejection capability. It is also important to mention that the PID controller optimized by the GA helped to obtain the desired response because this controller helps to guarantee the desired transient performance. Additionally, the Lyapunov theory used for designing the MRAC controllers guarantees closed-loop stability, with also fault-tolerant capability.

References

[1]   M. Blanke, M. Kinnaert, J. Lunze, and M. Staroswiecki, Diagnosis and Fault-Tolerant Control. 2nd ed. Springer-Verlag, 2006.
[2]   R. Isermann, Fault-Diagnosis Systems: An Introduction from Fault Detection to Fault Tolerance. Springer, 2006.
[3]   Y.M. Zhang and J. Jiang, "Bibliographical review on reconfigurable fault-tolerant control systems," Annual Reviews in Control, vol.32, no.2, pp. 229-252, Dec. 2008.
[4]   Z. Jiang, F. Li, W. Qiao, H. Sun, H. Wan, J. Wang, Y. Xia, Z. Xu, and P. Zhang, "A vision of smart transmission grids," Power and Energy Society General Meeting (PES), Calgary, July 26-30 2009, pp. 1-10.
[5]   J. Arai, K. Iba, T. Funabashi, Y. Nakanishi, K. Koyanagi, and R. Yokoyama, "Power electronics and its applications to renewable energy in Japan," IEEE Circuits and Systems Magazine, vol.8, no.3, pp. 52-66, 2008.
[6]   G. Fusco and M. Russo, "Adaptive voltage regulator design for synchronous generator," IEEE Transactions on Energy Conversion, vol.23, no.3, pp. 946-956, Sept. 2008.
[7]   F. Giuseppe and R. Mario, "Nonlinear control design for excitation controller and power system stabilizer," Control Engineering Practice, vol.19, pp. 243-251, 2011.
[8]   R.S. Munoz-Aguilar, A. Doria-Cerezo; E. Fossas, R. Cardoner, "Sliding mode control of a stand-alone wind rotor synchronous generator," IEEE Transactions on Industrial Electronics, vol.58, no.10, pp.4888-4897, Oct. 2011.
[9]   B.S. Kumar, S. Mishra, C.N. Bhende, M.S. Chauhan, "PI controller based frequency regulator for distributed generation," IEEE Region 10 Conference, pp.1-6, 19-21 Nov. 2008.
[10] S.-H. Lee, J.-S. Yim, J.-H. Lee, and S.-K. Sul. "Design of speed control loop of a variable speed diesel engine generator by electric governor," In IEEE Industry Applications Society Annual Meeting, 2008. pp. 1-5, Oct. 2008.
[11] Y. Duan, Y. Gong, Q. Li, and H. Wang, "Modelling and simulation of the microsources within a microgrid," In International Conference on Electrical Machines and Systems, pp. 2667-2671, Oct. 2008.
[12] R.S. Munoz-Aguilar, A. Doria-Cerezo, E. Fossas, and R. Cardoner, "Sliding mode control of a stand-alone wound rotor synchronous generator," IEEE Transactions on Industrial Electronics, vol.58, no.10, pp. 4888-4897, Oct. 2011
[13] J.P. Lyons, Wind Energy Systems, CTO Personal Communication, Novus Energy Partners, 2009.
[14] E.S. Abdin, and W. Xu, "Control design and dynamic performance analysis of a wind turbine-induction generator unit," IEEE Transactions on Energy Conversion, vol.15, no.1, pp. 91-96, Mar 2000.
[15] R. Abbas, F. Abdal and M. A. Abdulsada, "Simulation of wind turbine speed control by Matlab," International Journal of Computer and Electrical Engineering, vol.2, no.5, pp. 912-915, Oct. 2010.
[16] J. Chiasson and B. Vairamohan, "Estimating the state of charge of a battery," Proceedings of the 2003 American Control Conference, pp. 2863-2868, 4-6 June 2003.
[17] S. Pang, J. Farrell, J. Du, and M. Barth, "Battery state-of-charge estimation," Proceedings of the 2001 American Control Conference, pp.1644-1649, 2001.
[18] R. Carter, A. Cruden, P.J. Hall, and A.S. Zaher, "An improved lead acid battery pack model for use in power simulations of electric vehicles," IEEE Transactions on Energy Conversion, vol.27, no.1, pp. 21-28, March 2012.
[19] I. Minchala, L. Garza, and E. Calle, An intelligent control approach for designing a low voltage DC breaker, Proceedings of Innovation, Science and Society: Engineering for the Benefit of Humanity, Nov. 2012.
[20] L. I. Minchala-Avila, A. Vargas-Martínez, Y.M. Zhang, L. E. Garza-Castañón, E. R. Calle Ortiz and J. César Viola, "Model-based control approaches for optimal integration of a hybrid wind-diesel power system in a microgrid," Accepted in the 2nd International Conference on Smart Grids and Green IT Systems, Aachen, Germany, May, 2013.
[21] K. Astrom and B. Wittenmark, Adaptive Control, 2nd Edition, Addison-Wesley Publishing Company, 1995.
[22] I. J. Nagrath and M. Gopal, Control Systems Engineering, Indian Institute of Technology, Delhi, India: Anshan Ltd, 2006.
[23] A. Vargas-Martínez, L. E. Garza-Castañón, V. Puig and R. Morales-Menéndez, "Fault tolerant control for a second order LPV system using adaptive control methods," Proceeding of 5th Symposium on System Structure and Control Part of 2013 IFAC Joint Conference SSSC, Grenoble, France, pp. 852-857, Feb. 2013.
[24] L. E. Garza-Castañón and A. Vargas-Martínez. Artificial Intelligence Methods in Fault Tolerant Control, Chapter of Book Automation and Control-Theory and Practice, Ed. In-TECH, Austria, 2010.